

CrystEngComm

Accepted Manuscript



This is an *Accepted Manuscript*, which has been through the Royal Society of Chemistry peer review process and has been accepted for publication.

Accepted Manuscripts are published online shortly after acceptance, before technical editing, formatting and proof reading. Using this free service, authors can make their results available to the community, in citable form, before we publish the edited article. We will replace this *Accepted Manuscript* with the edited and formatted *Advance Article* as soon as it is available.

You can find more information about *Accepted Manuscripts* in the [Information for Authors](#).

Please note that technical editing may introduce minor changes to the text and/or graphics, which may alter content. The journal's standard [Terms & Conditions](#) and the [Ethical guidelines](#) still apply. In no event shall the Royal Society of Chemistry be held responsible for any errors or omissions in this *Accepted Manuscript* or any consequences arising from the use of any information it contains.

**Axis Symmetry of Silicon Molten Zone Interface Shape under
Mirror-Shifting-Type Infrared Convergent-Heating
Floating-Zone Method**

Md. Mukter Hossain,^a Satoshi Watauchi,^{*ab} Masanori Nagao^a and Isao Tanaka^a

^a *Center for Crystal Science and Technology, University of Yamanashi, 7-32 Miyamae, Kofu,
Yamanashi 400-8511, Japan*

^b *Precursory Research for Embryonic Science and Technology (PRESTO), Japan Science and
Technology Agency (JST), 4-1-8 Honcho, Kawaguchi, Saitama 332-0012, Japan*

^{*}*E-mail: watauchi@yamanashi.ac.jp*

Abstract

The shape of the silicon crystal, whether spiral or cylindrical, grown using the infrared convergent heating floating zone method, and the stability of the molten zone depend on the position of the mirror-lamp (M-L) system with respect to the grown crystal and molten zone. Through experiment, we studied the changes to the molten zone shape: the melt/feed, melt/gas, and melt/crystal interface shapes of the silicon molten zone under different positions of the M-L system. Although conventional parameters such as convexities (h/r) of the interface toward the melt were found to be independent of the position of the M-L system, the asymmetry of the zone length, L , was found to be inversely proportional to the distance of the M-L system from the center of the molten zone. A spiral crystal would be grown in this case. We introduce some parameters such as growth interface angle (δ), triple point angle (TPA), meniscus angle (MA), and altitude of the interface curvature (a_C) to characterize the axis symmetry of the melt/gas and melt/crystal interfaces. The variations in TPA, MA, and a_C were significantly reduced when the M-L system was shifted to a distant position from the center of the molten zone. On the other hand, the variations in δ were independent of the position of the M-L system. Thus, a symmetric molten zone was observed when the M-L system was at a distant rather than a close position. These behaviors were validated

through observations of the molten zone stability and the crystal shape.

Introduction

The floating-zone (FZ) method is a zone melting method that was developed by W. G. Pfann in the 1940s.¹ It is an effective method for growing single crystals from a melt, similar to the pulling and Bridgman methods.² There are several types of heat sources that can be used to form the molten zone: resistance heaters, induction coil heaters, and infrared convergent heaters are some. The infrared convergent-heating FZ (IR-FZ) technique uses a combination of an infrared lamp and an ellipsoidal mirror as an infrared convergent heater. This technique is used to grow dislocation-free silicon single crystals.³ Further, the grown silicon crystal is free from the contamination from crucible materials and heaters because this is also a crucible-free zone melting method.¹ Therefore, the grown crystal can be expected to have low oxygen and carbon content, as well as a long minority carrier lifetime.

However, the IR-FZ method is not suitable for industrial scale growth because the diameter of crystals grown is limited. It is about 15 mm at most, which is much smaller than that of the crystals grown by the Czochralski (CZ) and radio frequency heating FZ (rf-FZ) methods.³ In this study, a double ellipsoidal mirror type furnace was used for crystal growth. We confirmed that the behavior of the grown crystals remained the same when using a four ellipsoidal mirror type furnace.⁴ The diameter of the

cylindrically shaped crystal was ~20 mm, at most. In the trial to grow a crystal greater than ~20 mm in diameter, the shape of the grown crystal was spiral. The molten zone instability, which influences the contact between the feed and grown crystal, the drop of the melt, and the separation of the melt zone, prevents cylindrical growth in the conventional IR-FZ method. Crystals with diameters greater than ~20 mm exhibited a higher instance of molten zone instability even when carefully controlling the feed and grown crystal setting before growth and the lamp power operation were employed during growth.

Several studies on spiral growth in oxide materials with high melting points (typically above 1800 °C) in the CZ method have been conducted.⁵⁻⁷ It is also reported that, in the rf-FZ method, a lower melting point and lower radiative heat loss reduce melt stability, causing the growth of screw-like germanium crystals.⁸ However, no such studies have been reported on the spiral growth of silicon crystal in the IR-FZ method.

In IR-FZ growth, the stability of the molten zone is closely related to the heat flow, the interface shapes, and the grown crystal morphology.^{4,9-11} It has been reported that the growth diameter of the rutile crystal has been increased by tilting the convergent heating mirror. Further, this was closely related to the change in the shape of the melt/crystal interface.⁹ Rutile melt stability was enhanced in this manner.¹⁰ The shape of

the interface between the rutile crystal and melt zone is also affected by the rotation rate, as reported by Higuchi and Kodaira.¹² Some authors have noted that the interface shape can also be controlled using a heat reservoir.¹³⁻¹⁵

The interface shape of the molten zone for the cylindrical silicon crystals of 20 mm ϕ by the IR-FZ method has already been studied.¹⁶ It was noted that the position of the M-L system was systematically changed in the study; however, the conventional parameters characterizing the interface of the melt such as the zone length (L) and the convexity (h/r) of the interface between the grown crystal and the molten zone were found to be independent of the system position.

As we previously reported, the shape of the grown crystals, spiral or cylindrical, was significantly affected by the M-L system position and the size of the crystal grown.⁴ All 20 mm ϕ silicon crystals were cylindrical and independent of the M-L system position. On the other hand, the shapes of the crystals larger than ~ 20 mm in diameter were significantly affected by the M-L system position. When the M-L system was close, the crystals were spiral-shaped but when the M-L system was distant, the crystals were cylindrical-shaped. It follows then that the behavior of the 30 mm ϕ crystal interface shapes during IR-FZ growth would be different from that of the 20 mm ϕ crystal.

An axially symmetric molten zone is usually observed during the growth process when a grown crystal is cylindrical-shaped. However, the axis symmetric molten zone is absent when a spiral crystal is grown. The axis symmetry of the molten zone shape¹⁷ can also be coupled with the molten zone stability. Therefore, it must be important to study the axis symmetry of the interface shape during crystal growth.

In this study, the interface shape of the molten zone was carefully characterized. The conventional parameters of h/r for both the feed side and the crystal side, which are often used to discuss the shape of the interface, will not suffice to discuss the axis symmetry of the melt/gas interface shape. Thus, we introduce some parameters characterizing the axis symmetry of the molten zone: growth interface angle (δ), triple point angle (TPA), meniscus angle (MA), and altitude of interface curvature (a_C). These parameters are defined later in a figure. The dependence of these parameters and the size of the grown crystal on the position of the M-L system will be discussed.

Experimental section

A four-ellipsoidal-mirror-type image furnace (model FZ-T-10000-H-TY-1, Crystal Systems Corporation) was modified for this study. The ellipsoidal M-L systems could be moved towards or away horizontally along the radial direction from the center of the molten zone, where the rotation axes of the feed and grown crystal pass. The

position of each M-L system was shifted carefully using a screw gauge from -2 to +4 mm. After shifting, the M-L system was at equal distance from the rotation axis corresponding to the crystal center. By shifting the systems, the heat distribution at the surfaces of the feed, molten zone, and the grown crystal could be changed. A detailed explanation about M-L system position can be found in our earlier work.^{4,16} Tetragonal feed rods of $20 \times 20 \text{ mm}^2$ cross-sections were used in the experiments. Four 2.5 kW halogen lamps were used. The following growth parameters commonly used in both experiments are shown in Table I.

The feeding rate was gradually increased from 5 to 10 mm/h. After reaching the feeding rate of 10 mm/h, the growth experiment was continued for more than 1 h to achieve a constant growth diameter. During the experiment, the rotations and the positions of the feed and the seed crystal were set co-axially to provide axial thermal symmetry in the molten zone.

Polycrystalline cylindrical silicon was also used as seed crystal because the melt stability and interface shape of the bulk silicon crystal ($\sim 30 \text{ mm}\phi$) were mainly studied in these experiments. A small amount of iron powder ($\sim 0.15 \text{ g}$) was put on top of the seed crystal to form an iron-doped silicon molten zone. To examine the silicon molten zone shape, alternative experimental growth conditions and sample preparation

for characterization were required. These preparations were very similar to those previously reported.¹⁶ The characteristic parameters of the molten zone shape were determined using the iron distributions of the quenched molten zone and the photographs of the molten zone during the growth. The iron distributions of the quenched molten zone were examined using an electron probe micro-analyzer (EPMA; model JXA-8200, JEOL Ltd.). To comprehensively discuss the interface shapes, δ , TPA, MA, and a_C were determined from the EPMA mapping images in addition to the gap between the feed and the crystal (hitherto referred to as the gap) and h/r . MA and L were also determined from the photographs of the molten zone during the growth.

Results and discussion

Fig. 1 shows the photographs of the silicon crystal of 30 mm ϕ , the molten zone and the feed rod quenched during the growth at (a) -2, (b) +1, (c) +4, and (d) +6 mm position of the M-L system. Fig. 1 (a, b) shows spiral crystals, while Fig. 1 (c, d) shows cylindrical crystals. The more stabilized molten zone could be gradually realized when the position of the M-L system was moved from -2 to +6 mm position. These observations are consistent with our previous report.⁴

The photographs of the molten zone during crystal growth at the (a) -2, (b) +1,

(c) +4, and (d) +6 mm positions are shown in Fig. 2. The dash-dotted vertical and dashed horizontal lines indicate the rotation axis and the eye guide showing the line of the realization of an axis symmetric molten zone, respectively. The asymmetric melt/gas and melt/crystal interface shapes of the ~ 30 mm ϕ crystal are clearly observed in Fig. 2(a). More symmetric interface shapes gradually formed, which can be recognized in the photographs of the molten zone formed at the distant position of M-L system, as shown in Fig. 2(b-d). For quantitative analysis, the difference of the interface position is defined in Fig. 2 (a). The behavior of the difference of the interface position is shown in Fig. 3 as a function of the M-L position. The difference of interface position is almost zero when the M-L system is at +4 and +6 mm position.

Fig. 4 shows the EPMA mapping images of the quenched molten zone cross-section for the ~ 30 mm ϕ silicon crystal formed at differing M-L system position. Fig. 4 (a, b) exhibits spiral crystals, while Fig. 4 (c, d) shows cylindrical crystals. To characterize the molten zone shape as a function of the M-L position, the conventional parameters such as convexity (h/r), zone length (L), and gap are shown in Fig. 5. The definitions of these parameters are summarized in Fig. 5 (a). As we have already reported,¹⁶ the effects of lamp power on the interface shape should be excluded to discuss the effect of the M-L system position on the interface shape. The minimal steady

gap condition between the feed and grown crystal was a good way to avoid the lamp power effects on the interface shape. Therefore, minimal lamp power was applied during all growth experiments to avoid contact between the feed and grown crystal. The observed gap remained nearly constant at 3 mm, as shown in Fig. 5 (b). This meant that the effect of the lamp power on the interface shape could be ignored, allowing the observed results to be discussed based solely on the effects of the M-L system position.

As shown in Fig. 5 (b), the characteristic behavior of L for ~ 30 mm ϕ crystals, which are defined as the lengths of both left and right sides of the molten zone in the photograph (Fig. 2), was significantly different from that of the ~ 20 mm ϕ crystals.¹⁶ At -2 mm position of the system, the variations in L were clearly recognizable because of the difference in the melt/crystal interface position. At +4 and +6 mm position, the variations were significantly reduced. As shown in Fig. 5 (c), the h/r for both melt/feed and melt/crystal are independent of the M-L system position although the shapes of the grown crystals are significantly different. These behaviors for ~ 30 mm ϕ crystals are similar to those for ~ 20 mm ϕ crystals.¹⁶ But, the absolute values of the gap and h/r for ~ 30 mm ϕ crystal growth are different from those for ~ 20 mm ϕ crystal.¹⁶ The different values of these parameters can be attributed to the size. However, these results indicate the h/r may not be a good parameter to characterize the effects of M-L position on the

axis symmetry of the silicon molten zone.

As we mentioned above, the differences in the interface position and L are dependent on the position of M-L system, as shown in Fig. 3 and 5 (b). This implies that the axis symmetry of the molten zone shape is affected by the M-L position. Greater axis asymmetric molten zone shape can be clearly recognized at -2 mm position of the M-L system, as shown in Fig. 2. To investigate the change of axis symmetry of the molten zone, some characterizing parameters such as the growth interface angle (δ), triple point angle (TPA), meniscus angle (MA), and altitude of interface curvature (a_C) were introduced.¹⁸ These parameters are defined in Fig. 6. Recently, some of these parameters were found to be useful to discuss the stability of the molten zone.

Fig. 7 shows the behaviors of δ , TPA, MA, and a_C at the crystal-liquid-gas point as a function of the M-L system position. All the data, plotted as closed circles in Fig 7 (a-d), were obtained from the EPMA images shown in Fig. 4. The open circle data in Fig. 7 (c) were obtained using three photographs of the molten zone. Fig. 2 is an example of such photographs. Each image provides us two data points for each parameter, from the left and right sides of the crystal-liquid-gas point. The variations of δ for crystal growth in ~ 30 mm ϕ crystals were very small and these were almost independent of the of M-L system position, as shown in Fig. 7(a).

On the other hand, the differences in TPA, MA, and a_C were significantly decreased with the increase in the distance of the M-L system position, as shown in Fig. 7 (b-d). This indicates that the shape of the molten zone is more symmetric when the M-L system is more distant. The shape of the grown crystal was changed from spiral to cylindrical as the distance of the M-L system increased. The boundary position of the M-L system was around + 1 mm position. This suggests that there is a criterion of TPA or MA that determines whether the shape of the grown crystal is cylindrical or spiral.

20 mm ϕ crystals were grown as cylindrical at any position of the M-L system as we have previously reported.¹⁶ The differences of these parameters (δ , TPA, MA and a_C) for the 20 mm ϕ crystals are very small, and they are independent of the M-L position, although the figures are not shown. The differences in MA and TPA for the growth of 20 mm ϕ cylindrical crystals at any position of the M-L system are ~ 2 and $\sim 6^\circ$, respectively, which are still smaller than ~ 12 and $\sim 9^\circ$, respectively, at the + 1 mm boundary position for the growth of 30 mm ϕ spiral crystal. This scenario could be closely related with the shape of the grown crystal, whether spiral or cylindrical.

A possible reason for the asymmetric molten zone shape at the closer position of the M-L system could be the temperature gradient at the surface of the molten zone, which corresponds to the focusing of the convergent light. Generally, the focus position

of the M-L system is on the rotation axes of the molten zone in the conventional IR-FZ method, including when at the zero position of the M-L system in our experiment. The convergent infrared light is mainly absorbed at the surface of the molten zone. Thus, it follows that at closer position of the M-L system, the focusing of the convergent light cannot be sharp at the surface of the molten zone when the molten zone is thick. For a thick molten zone, optimum focusing at this surface can be achieved only at the more distant position of the M-L system. Our results indicate that a cylindrical crystal is grown at a sharper focusing condition, and that a spiral crystal is grown at a shallower focusing condition. A steeper temperature gradient at the surface of the molten zone along the axial direction is realized at a sharper focusing condition. Simulation works on the temperature fields in the molten zone along the radial direction caused by changing the positions of the lamps have already been studied by C. W. Lan *et. al.*¹⁹ Some effects of the position of M-L system in our present experiments are expected to be similar with those studies. They reported that the temperature fields are more uniform when the lamps are moved outwards from the foci and vice versa. Unfortunately, the temperature field along the axial direction was not mentioned.

The effects of the temperature gradient on the heat flow and on the stability of the convection have already been studied. The solid-melt interface in a floating zone

silicon melt was fluctuated by the temperature fluctuation induced by Marangoni convection.²⁰ This convection can lead to unstable heat flow and reduce the stability of the molten zone^{21,22} although in the silicon melt, conduction heat transfer is the dominant flow rather than convection due to the low Prandtl number of the silicon melt.²³⁻²⁵ The heat flow along the azimuthal direction is relatively effective when the temperature gradient along the axial direction is decreased.²⁶ The asymmetric heat flow along the azimuthal direction is realized there. The asymmetric bulge observed in the growth for closer position of the M-L system might be on account of the asymmetric heat flow. However, some authors have also studied the growth angle and meniscus angle of silicon crystals grown during the rf-FZ and CZ methods.^{17,27} However, the mechanism of the position effects on the shape of the grown crystal is not fully clear yet. For further discussion about this, the position of M-L system dependence simulation works on the melt convection and the temperature distribution in the molten zone is important. Unfortunately, no clear theoretical data for the growth of IR-FZ method is available to compare with our results.

Conclusions

The shape of the silicon molten zone during infrared convergent heating

floating zone growth was characterized. The convexity (h/r), one of the conventional parameters characterizing the molten zone shape, was found to be insufficient to discuss the change of melt/gas and melt/crystal interface shapes of the molten zone as a function of the M-L system position. Therefore, some characteristic parameters, the growth interface, triple point, and meniscus angles (δ , TPA, and MA, respectively) and altitude of the interface curvature, a_C , were introduced. The variation in δ was independent of M-L position. On the other hand, the variations in TPA, MA, and a_C were found to depend on the M-L system position. These variations decreased at the more distant positions of the M-L system and vice versa. At distance position of the M-L system, cylindrical crystals were grown. These observations imply that the axis symmetry of the melt/gas and melt/crystal interface shapes, which can be controlled by position of the M-L system, can determine the shape of the grown crystal. Both experimental and simulation works on the convection flow are required before further discussions to explain the dependence of the formed molten zone shape on the position of the M-L system in a mirror-shifting type IR-FZ furnace.

Acknowledgements

This work was partially supported by the Japan Science and Technology Agency (JST), Precursory Research for Embryonic Science and Technology (PRESTO).

References

- 1 W. G. Pfann, *Trans. Am. Inst. Min. Metall. Eng.*, 1952, **194**, 747-753.
- 2 S. M. Koohpayeh, D. Fort and J. S. Abell, *Prog. Cryst. Growth Charact. Mater.*, 2008, **54**, 121–137.
- 3 A. Eyer, B. O. Kolbesen and R. Nitsche, *J. Cryst. Growth*, 1982, **57**, 145–154.
- 4 M. M. Hossain, S. Watauchi, M. Nagao and I. Tanaka, *Cryst. Growth & Des.*, 2014, **14**, 5117–5121.
- 5 R. Uecker, H. Wilke, D. G. Schlom, B. Velickov, P. Reiche, A. Polity, M. Bernhagen and M. Rossberg, *J. Cryst. Growth*, 2006, **295**, 84–91.
- 6 J. -P. Chaminade, O. Viraphong and S. Miyazawa, *J. Cryst. Growth*, 2002, **237–239**, Part 1, 864–868.
- 7 D. Schwabe, R. Uecker, M. Bernhagen and Z. Galazka, *J. Cryst. Growth*, 2011, **335**, 138–147.
- 8 M. Wünscher, A. Lüdge and H. Riemann, *J. Cryst. Growth*, 2011, **318**, 1039–1042.
- 9 M. A. R. Sarker, S. Watauchi, M. Nagao, T. Watanabe, I. Shindo and I. Tanaka, *J. Cryst. Growth*, 2011, **317**, 135–138.
- 10 S. Watauchi, M. A. R. Sarker, M. Nagao, I. Tanaka, T. Watanabe and I. Shindo, *J. Cryst. Growth*, 2012, **360**, 105–110.

- 11 M. A. R. Sarker, S. Watauchi, M. Nagao, T. Watanabe, I. Shindo and I. Tanaka, *J. Cryst. Growth*, 2010, **312**, 2008–2011.
- 12 M. Higuchi and K. Kodaira, *Mater. Res. Bull.* 1994, **29**, 545–550.
- 13 M. A. Gonik and A. Cröll, *CrystEngComm*, 2013, **15**, 2287–2293.
- 14 K. Kitamura, S. Kimura and K. Watanabe, *J. Cryst. Growth*, 1982, **57**, 475–481.
- 15 S. Watauchi, I. Tanaka, K. Hayashi, M. Hirano and H. Hosono, *J. Cryst. Growth*, 2002, **237–239**, Part 1, 801–805.
- 16 M. M. Hossain, S. Watauchi, M. Nagao and I. Tanaka, *CrystEngComm*, 2014, **16**, 4619–4623.
- 17 M. Wünscher, A. Lüdge and H. Riemann, *J. Cryst. Growth*, 2011, **314**, 43–47.
- 18 M. M. Hossain, S. Watauchi, M. Nagao and I. Tanaka, *J. Cryst. Growth*, 2016, **433**, 24–30.
- 19 C. W Lan, C. H. Tsai, *J. Cryst. Growth*, 1997, **173**, 561–573.
- 20 M. Sumiji, S. Nakamura and T. Hibiya, *J. Cryst. Growth*, 2002, **235**, 55–59.
- 21 C. W Lan, S. Kou, *J. Cryst. Growth*, 1991, **108**, 351–366.
- 22 C. W Lan, *J. Cryst. Growth*, 2003, **247**, 597–612.
- 23 N. Kobayashi, *J. Cryst. Growth*, 1984, **66**, 63–72.
- 24 N. Kobayashi and W. R. Wilcox, *J. Cryst. Growth*, 1982, **59**, 616–624.

- 25 C. E. Chang and W. R. Wilcox, *Int. J. Heat Mass Transfer*, 1976, **19**, 355–366.
- 26 S. Nakamura, T. Hibiya, K. Kakimoto, N. Imaishi, S. Nishizawa, A. Hirata, K. Mukai, S. Yoda and T. S. Morita, *J. Cryst. Growth*, 1998, **186**, 85–94.
- 27 T. Surek and B. Chalmers, *J. Cryst. Growth*, 1975, **29**, 1–11.

Table**Table I.** Growth conditions

Feed dimensions (mm ²)	20×20
Feeding rate (mm/h)	10
Growth rate (mm/h)	5
Shaft rotation (Upper/lower) (rpm)	6/15
Crystal diameter (mm)	30
Vacuum level (Pa)	3×10^{-3}
Growth atmosphere	Ar flow 1 L/min

Figure captions

Fig. 1. Photographs of quenched silicon crystal of 30 mm ϕ prepared at (a) -2, (b) + 1, (c) +4, and (d) +6 mm position of mirror-lamp (M-L) system. Note here that (a, b) shows a spiral crystal while (c, d) shows a cylindrical crystal.

Fig. 2. Photographs of the molten zone indicating the melt/gas and melt/crystal axis asymmetry and symmetry for different mirror-lamp (M-L) system positions: (a) -2 and (b) +1 mm, which both indicate asymmetry, and (c) +4 and (d) +6 mm, which both indicate symmetry. The dash-dotted vertical lines indicate the rotation axes, and the dashed horizontal lines are the eye guide showing the visualization line of the axisymmetric melt/gas and melt/crystal interface shapes.

Fig. 3. The difference in the crystal-melt interface position as a function of the position of mirror-lamp (M-L) system. The dash-dotted lines indicate the focus positions of the M-L systems on the rotation axes of the feed and grown crystals.

Fig. 4. Iron-distributed mapping images of the cross-section of the quenched molten zone prepared at the different M-L system positions: (a) -2, (b) +1, (c) +4, and (d) +6 mm.

Fig. 5. Behaviors of the characteristic parameters of the molten zone interface shape. Specifically, the (a) schematic diagram of the molten zone showing the definition of

convexity (h/r), gap, and zone length, L (b) gap and the zone length (L), (c) convexity (h/r) as a function of the M-L system position. Note that the values of L are obtained from both edge lengths of the molten zone using photographs shown in Fig. 2, and that the values of the gap and h/r are obtained from the EPMA images shown in Fig. 4. The dash-dotted lines indicate the focus positions of the M-L systems on the rotation axes of the feed and the grown crystal.

Fig. 6. Schematic illustration of the molten zone showing the definition of some characteristic parameters such as growth interface angle (δ), triple point angle (TPA), meniscus angle (MA), and altitude of interface curvature (a_c).

Fig. 7. Variations in the parameters characterizing the axis symmetry of the melt/gas and melt/crystal interface shapes. Here (a) growth interface angle (δ), (b) triple point angle (TPA), (c) meniscus angle (MA), and (d) altitude of interface curvature (a_c) as functions of M-L system position are shown for ~ 30 mm ϕ crystals at the crystal-liquid-gas point. The closed circle data were determined from the EPMA images shown in Fig. 4. The open circle data in (c) were obtained from the three photographs of the molten zone during growth. The dash-dotted lines indicate the focus positions of the M-L systems on the rotation axes of the feed and grown crystals.

Figures

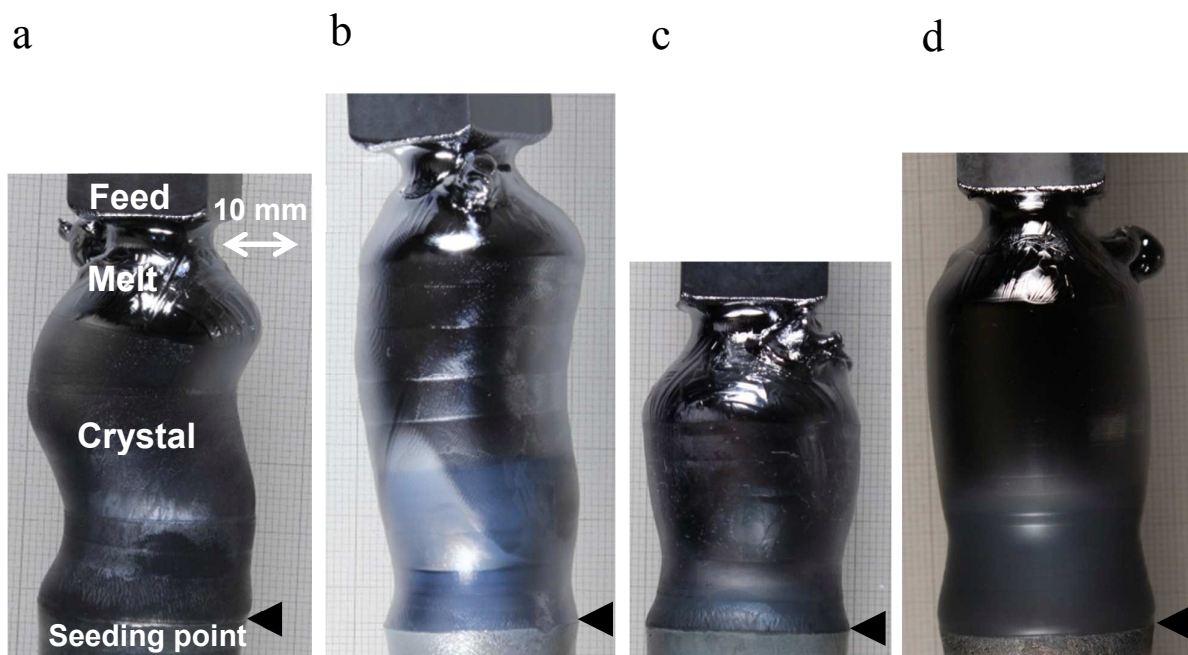


Fig. 1. (Hossain et al.)

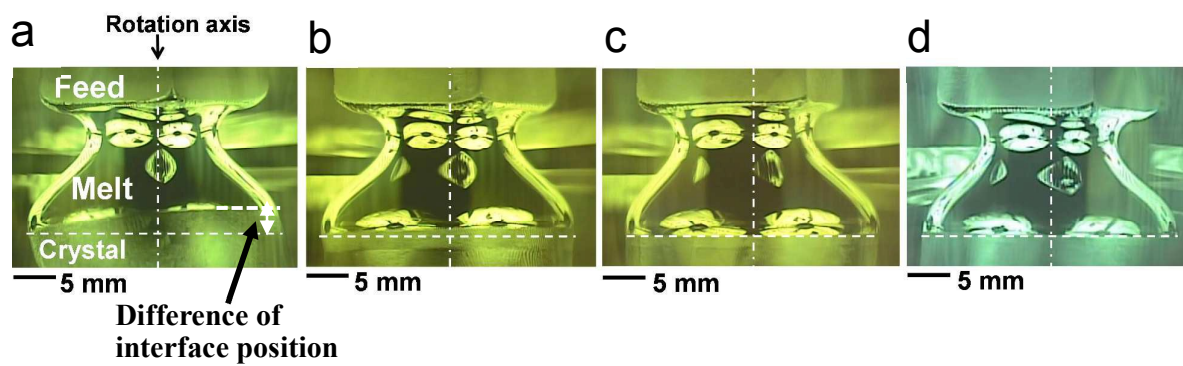


Fig. 2. (Hossain et al.)

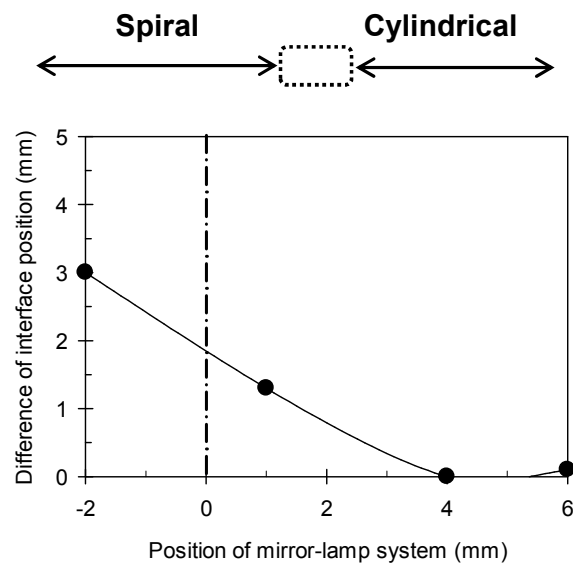


Fig. 3. (Hossain et al.)

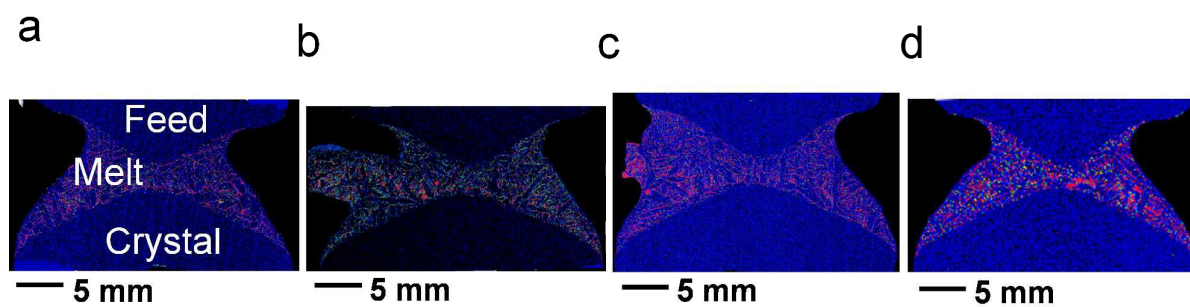


Fig. 4. (Hossain et al.)

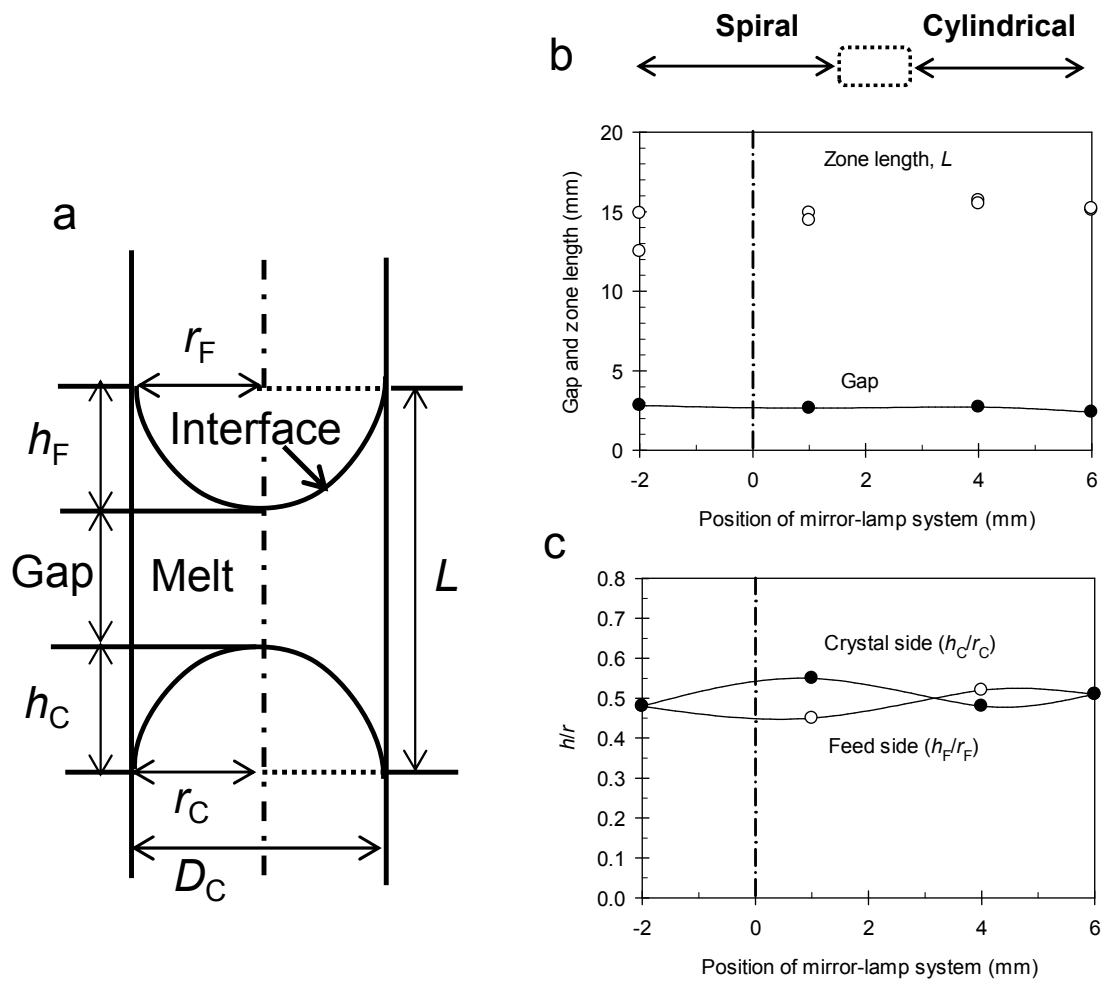


Fig. 5. (Hossain et al.)

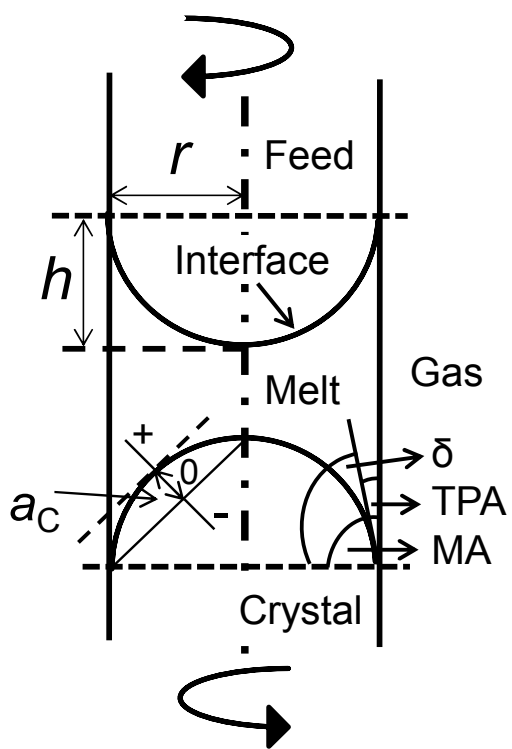


Fig. 6. (Hossain et al.)

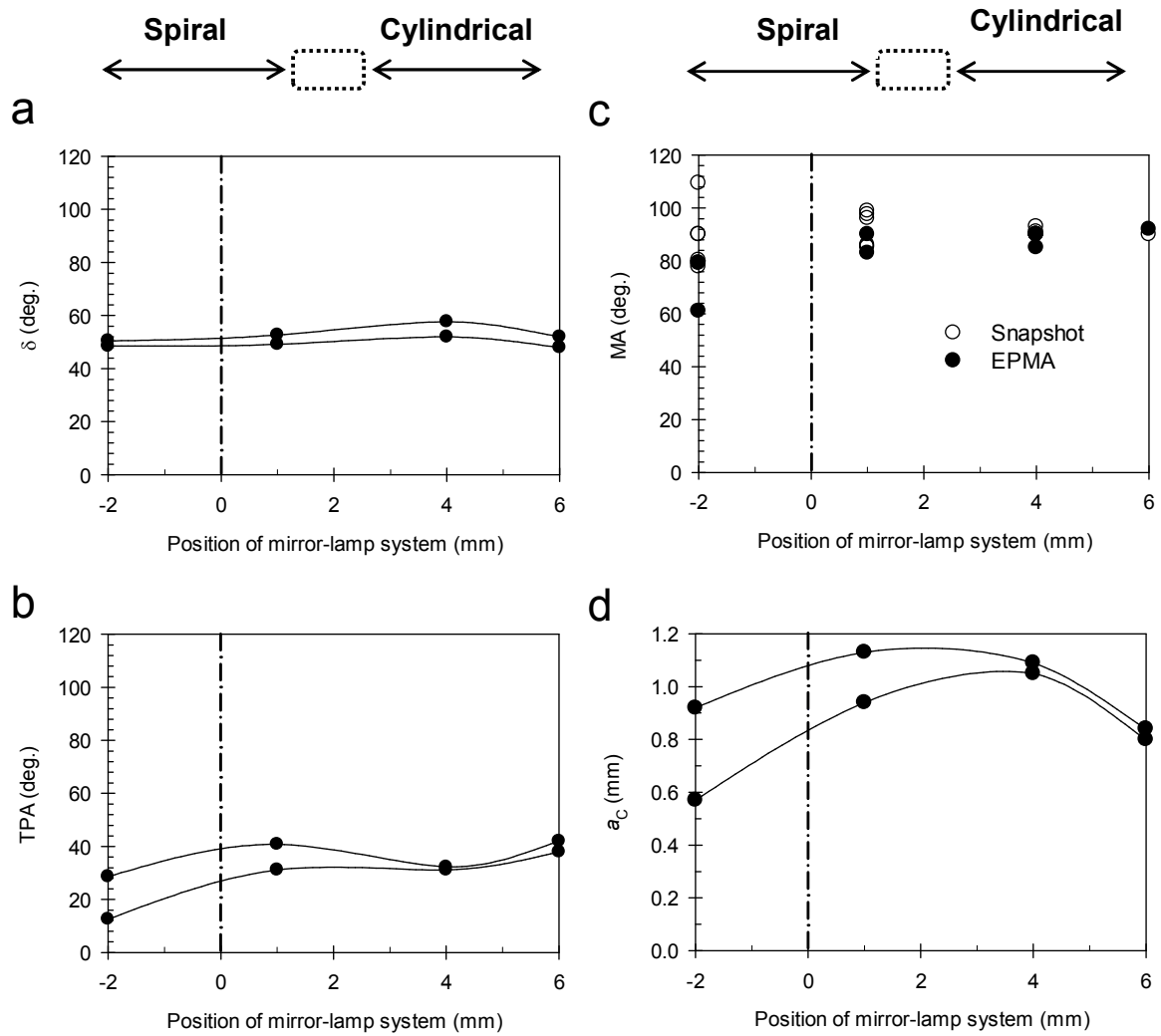
**Fig. 7.** (Hossain et al.)

Table of Contents (TOC):

Axis symmetry of silicon molten zone shape, which is depended on the position of mirror-lamp (M-L) system, is related with the shape of the grown crystal.

